AIChE

New Insights on Mass Transfer Kinetics in Chromatography

Fabrice Gritti and Georges Guiochon
Dept. of Chemistry, University of Tennessee, Knoxville, TN 37996

DOI 10.1002/aic.12271
Published online May 4, 2010 in Wiley Online Library (wileyonlinelibrary.com).

The mass transfer kinetics of thiourea, phenol, ethylbenzene, propylbenzene, butylbenzene, and amylbenzene were studied on a Gemini-C_{18} (5 μm, 110 Å, 375 m^2/g) column (150 mm × 4.6 mm) eluted with methanol/water solutions (100, 90, and 20% v/v). Each of the successive steps of the mass transfer of these solutes (axial diffusion, eddy dispersion, film mass transfer resistance, and transparticle mass transfer resistance) was unambiguously measured, using a combination of the peak parking method, the total pore blocking method, and moment analysis, in a wide range of reduced linear velocities. The results obtained offer new insights on the mass transfer kinetics in chromatographic columns. They show first that the eddy dispersion A-term is strongly correlated with the particle porosity. The complex, anastomosed transcolumn flow pattern causes extra band broadening. This transcolumn effect was found to be markedly smaller with porous particles than with nonporous particles of the same size. Second, the film mass transfer coefficient of retained compounds is smaller for porous than for nonporous particles, a result consistent with concentration gradients being steeper at the wall of solid particles than across the entrance surface of pores. The external mass transfer coefficient decreases with increasing fraction of the surface area of the particles that is open to pores, e.g., with increasing particle porosity. *AIChE J*, 57: 333–345, 2011
Keywords: liquid chromatography, column efficiency, mass transfer kinetics, parking experiments, longitudinal diffusion coefficient, particle diffusivity, total pore blocking experiments, eddy dispersion, solid–liquid mass transfer resistance, film mass transfer, Sherwood number, transparticle mass transfer resistance

Introduction

Over forty years ago, Giddings established the fundamentals of the mass transfer mechanisms in chromatography.[1] Using a statistical approach, he derived the main equations accounting for axial diffusion at zero or finite flow velocities, eddy dispersion, and for the resistance to mass transfer between the stationary and the mobile phases. Although Giddings theory of band broadening did not take into consideration the detailed structure of the adsorbent, his work included the dynamics of gas and liquid chromatography.

Later, more sophisticated approaches such as the general rate model were developed, involving characteristic properties of packed beds like the properties of the solid particles, and introduced two mass balance equations, one for the mobile phase percolating through the bed, the other for the stagnant eluent inside the porous particles.[2] These equations were solved in the Laplace domain.[3] The general rate model was later extended to different geometries of the adsorbent bed, i.e., to beds packed of partially or fully porous spherical particles or to beds of monolithic columns that are filled of networks of lumps of porous silica.[4] Still, using this model

Correspondence concerning this article should be addressed to G. Guiochon at guiochon@utk.edu.

needs to assume the validity of some conventional correlations that provide the axial dispersion in the mobile phase[2] and/or the film mass transfer resistance,[5,6] correlations which have not always been validated at the scale of chromatographic beds nor at the level of accuracy at which chromatographic parameters can be measured.

It has not been possible to validate any of these correlations because the available methods of analyzing band broadening phenomena cannot target selectively one of the different mass transfer contributions among the others. Miyabe et al.[7] used nonporous particles to eliminate the transparticle mass transfer resistances. They isolated the film mass transfer resistance term and found a good agreement between their value of the film mass transfer coefficient, k_f, and those yielded by available correlations based on data measured with nonporous materials. Still, they did not check whether the porosity has an effect on k_f nor if the correlations do apply to porous particles as commonly assumed in liquid chromatography. The same argument holds regarding the eddy dispersion term. A priori, the coupling theory of eddy dispersion of Giddings suggests that whether particles are porous or not should have no influence on the eddy dispersion term of any compound. This assumption needs to be checked out, using appropriate experimental data.

To answer these questions, we have developed an experimental protocol that allows the separate determination of each one of the kinetic steps taking place in chromatographic columns. These experiments combine the peak parking method, the total pore blocking method and moment analysis. If small samples are used, the peak parking method permits the direct and accurate measurement of particle diffusivity.[8,9] The total pore blocking method[10] measures accurately the external porosity of LC columns and gives access to the eddy dispersion term. We applied this protocol to a commercial column (Gemini-C_{18}), using samples of thiourea, phenol, ethylbenzene, propylbenzene, butylbenzene, and amylbenzene. The values of each of the mass transfer terms will be discussed in detail, based on the experimental results, and compared with those given by correlations available in the literature.

Theory

Definitions

The following terms will be employed in this work.

- The particle diffusivity D_p measures the effective diffusion coefficient of a compound inside individual particles of the packing material. By definition, this diffusion coefficient takes the concentration gradient in the pores as the driving force,[11] consistent with the definition of the effective particle diffusivity in the general rate model of chromatography.[2] It results from the combination of pore and surface diffusion. The ratio of D_p and the molecular diffusivity, D_m, of the compound in the bulk mobile phase is Ω.
- The axial diffusion coefficient $D_{eff}(v = 0)$ of a compound is its effective diffusion coefficient inside the packed bed, at a zero velocity. It results from the combination of its diffusion in the interstitial column volume (D_m) and the particle diffusivity (D_p).
- The transparticle and the film mass transfer coefficients C_p and C_f of the general reduced plate height model are derived from the moments of the Laplace transform of the general rate model mass balance equations,[3,4,12] assuming that the packed particles are spherical.

General HETP equation for chromatographic columns

The broadening of a band migrating along an isothermal chromatographic column is due to the simultaneous influence of a series of independent elementary steps. From a phenomenological point of view, Giddings discussed in detail each of these mass transfer steps and provided the fundamentals of band broadening in liquid chromatography.[1] These steps are axial diffusion of the band in the absence of flow or in the mobile phase reference framework, eddy dispersion in the interstitial void volume (interparticle space), mass transfer resistance through the thin film of eluent that is between the eluent percolating the interstitial column volume and the stagnant eluent inside the porous adsorbent particles, the mass transfer resistance between the two eluents, the mass transfer resistance through the particles, and the kinetics of adsorption-desorption (this latter kinetics is usually very fast with small molecules, hence its contribution is neglected). These different terms are accounted for by corresponding contributions to the general rate model.[2] In the linear case, the set of mass balance equations of this model can be solved in the Laplace domain. However, this solution cannot be transformed back to the time domain but its moments can. This provides the moments of the chromatographic band at column outlet.[3] Application of this mathematical strategy was extended to other chromatographic bed structure (e.g., beds packed of fully, partially, or nonporous particles and monolithic beds). It lead to specific expressions valid in these cases.[4] As longitudinal diffusion and eddy dispersion can be considered as independent kinetic phenomena, the overall reduced HETP of an isothermal column packed with fully porous spherical particles can be written as follows:[1,2]

$$h(v) = \frac{2D_{eff}(v)}{v} + h_{eddy}(v) + \frac{1}{30}\frac{\varepsilon_e}{1-\varepsilon_e}\left(\frac{\delta_0}{1+\delta_0}\right)^2\frac{1}{\Omega}v + \frac{1}{3}\frac{\varepsilon_e}{1-\varepsilon_e}\left(\frac{\delta_0}{1+\delta_0}\right)^2\frac{D_m}{k_f d_p}v \quad (1)$$

$$= \frac{2D_{eff}(v)}{v} + h_{eddy} + C_p v + C_f v \quad (2)$$

$$= \frac{2D_{eff}(v)}{v} + h_{eddy} + C_h v \quad (3)$$

where $D_{eff}(v)$ is the longitudinal diffusion coefficient, a function of the linear reduced velocity, v, $h_{eddy}(v)$ is the eddy dispersion term, ε_e is the interstitial porosity of the column, d_p is the average particle size, and k_f is the film mass transfer coefficient between the solid phase surface and the mobile phase. $\frac{k_f d_p}{D_m}$ is the dimensionless Sherwood number. The reduced interstitial linear velocity v is defined as:

$$v = \frac{u d_p}{D_m} \quad (4)$$

where u is the local interstitial linear velocity.

The parameter δ_0 in Eq. 1 is written:

$$\delta_0 = \frac{1-\varepsilon_e}{\varepsilon_e}\left[\varepsilon_p + (1-\varepsilon_p)K\right] \quad (5)$$

where ε_p is the porosity of the solid adsorbent and K is the Henry's constant of the compound considered:

$$K = \frac{\varepsilon_t}{1-\varepsilon_t}k' \quad (6)$$

where $\varepsilon_t = \varepsilon_e + (1-\varepsilon_e)\varepsilon_p$ is the total porosity of the bed and k' is the compound retention factor:

$$k' = \frac{V_R - V_0}{V_0} \quad (7)$$

where V_R is the elution volume of the sample and V_0 the hold-up volume of the column derived from pycnometric data, see results in "Materials" Section.

The main goal of this work is to develop an experimental protocol providing direct, clear values of D_{eff}, Ω, h_{eddy}, and k_f in Eq. 1. This would eliminate the need of making many conventional assumption and/or of using other correlation equations than the Wilke and Chang equation,[13] which provides reasonable estimates of the diffusion coefficient D_m of small analytes in the mobile phase[14,15]:

$$D_m = \frac{7.4\ 10^{-8}\sqrt{x_A\phi_A M_A + x_B\phi_B M_B}\ T}{\eta_{AB}V_b^{0.6}} \quad (8)$$

where x_A and x_B, ϕ_A and ϕ_B, M_A and M_B are the molar fractions, the associative factors (1.9 for methanol, 2.6 for water), and the molecular weights (g/mol) of the two solvents A and B used (32 g/mol for methanol, 18 g/mol for water), respectively, η_{AB} is the viscosity (cP) of the binary eluent listed in,[2] and V_b is the molar volume of the compound considered at its boiling point, estimated from the LeBas group method.[14]

Note that independent experimental studies have shown that the values of D_m measured with the Aris-Taylor method using long widely coiled capillary tubes ($\simeq$15-m long, $\simeq$0.5-mm internal diameter) kept at constant temperature differs by less than $\pm$10% from the Wilke and Chang estimate.[15]

Moment analysis and reduced column HETP

The processes of data acquisition and calculations was kept exactly the same for the three series of measurements performed: those of the moments of the extra-column volume of the instrument, of the column operated under its standard configuration (pores unblocked), and of the column operated after blocking its mesopores. The first moment (μ_1) and the second central moment (μ'_2) of the bands were derived by integration of the recorded signal:

$$\mu_1 = \frac{\int_0^\infty C(t)t\,dt}{\int_0^\infty C(t)t\,dt} \quad (9)$$

$$\mu'_2 = \frac{\int_0^\infty C(t)(t-\mu_1)^2 dt}{\int_0^\infty C(t)dt} \quad (10)$$

For this calculation, the experimental baseline was first corrected to obtain an horizontal base line at $C = 0$. The peaks were cut on their left side, slightly before the shock layer and on their right side at the time corresponding to the elution of 99.5% of the mass injected. This approach was systematically applied to all the peaks recorded in the absence and in the presence of the column, with the pores blocked or unblocked. The reproducibility of the measurements is better than 10%. Their precision can be assessed from the dispersion of the HETP data points in Figures 5 and 7.

The reduced column HETP h is determined using the following definition:

$$h = \frac{L}{d_p}\frac{\mu'_2 - \mu'_{2,ex}}{(\mu_1 - \mu_{1,ex})^2} \quad (11)$$

where L is the column length.

The relative error made on h is written:

$$\left|\frac{\Delta h}{h}\right| = \left|\frac{\Delta\mu'_2}{\mu'_2}\right|\left(\frac{\mu'_2 + \mu'_{2,ex}}{\mu'_2 - \mu'_{2,ex}}\right) + 2\left|\frac{\Delta\mu_1}{\mu_1}\right|\left(\frac{\mu_1 + \mu_{1,ex}}{\mu_1 - \mu_{1,ex}}\right) \quad (12)$$

The second and the first moments of the tracer peak, μ'_2 and μ_1, were measured successively five times, first with the chromatographic column fitted to the instrument, then after replacing the column with a zero-volume connector. The relative error made on these moments are always smaller than 5 and 0.5%, for the second and first moments, respectively. The first term between parentheses in the right-hand side of Eq. 12 varied between 1.21 and 1.61 when the mesopores were unblocked and between 1.28 and 1.66 when the mesopores were blocked. The second term between parenthesis varied between 1.04 and 1.06 when the mesopores were unblocked and between 1.09 and 1.11 when the mesopores were blocked. Accordingly, the largest possible systematic relative error made in the measurement of h was 9.2% when the mesopores were blocked.

Experimental

Chemicals

All the mobile phases used in this work were mixtures of water and methanol. Water, methanol, 2-propanol, dichloromethane, nonane, 85% phosphoric acid, and potassium dihydrogenphosphate were all purchased from Fisher Scientific (Fair Lawn, NJ) and used without further purification. The mobile phase was filtered before use on a surfactant-free cellulose acetate filter membrane, 0.2 μm pore size (Suwannee, GA). Thiourea, sodium nitrate, phenol, ethylbenzene, propylbenzene, butylbenzene, and amylbenzene, selected as injected samples, were also from Fisher Scientific.

Materials

The 150 mm × 4.6 mm endcapped Gemini-C_{18} (110 Å average pore size, 375 m^2/g specific surface area) and Sunfire-C_{18} (90 Å average pore size, 349 m^2/g specific surface area) columns used were gifts from the column manufacturers (Phenomenex, Torrance, CA, USA and Waters, Mildford, MA). All peaks eluted from the Gemini column exhibited slightly but systematically deformed profiles (slight peak fronting), an effect which was unambiguously attributed to packing heterogeneity (see discussion later). For the sake of comparison, the eddy dispersion data were also measured on the Sunfire column, which shows no peak fronting. The total porosity of the Gemini column bed was measured by pycnometry[16] at 20°C using methanol (density $\rho_{CH_3CN} = 0.791 \pm 0.001$ g/cm^3) and dichloromethane (density $\rho_{CH_3CN} = 1.326 \pm 0.001$ g/cm^3) as the two eluents. The masses of the column filled with methanol or dichloromethane were 66.60785 and 67.50600 ± 0.00005 g, respectively, giving $\varepsilon_t = 0.673 \pm 0.003$. The external porosities of the Gemini and Sunfire columns ($\varepsilon_e = 0.364$ and 0.347 ± 0.001, respectively) were determined from the results of the total pore-blocking experiments,[10] using sodium nitrate as the unretained compound.

Apparatus

The measurements were made with a HP1090 liquid chromatograph series II (Hewlett-Packard, Palo Alto, CA). This instrument includes a ternary solvent delivery system, an auto-sampler with a 250 μL sample loop, a diode-array UV detector (cell volume 1.7 μL, sampling rate 25 Hz), a column air-oven, and a data station. From the exit of the Rheodyne injection valve to the column inlet and from the column outlet to the detector cell, the total extra-column volume of the instrument is 46 μL, measured as the apparent hold-up volume of a zero-volume union connector in place of the column. The flow-rate delivered by the three pumps was measured at column outlet, under atmospheric pressure. During the HETP measurements, the flow rates were fixed at 0.10, 0.25, 0.50, 0.75, 1.00, 1.50, 2.00, 2.50, and 3.00 mL/min. The maximum inlet pressure recorded was around 300 bar at 3.0 mL/min for both Gemini and Sunfire columns using the two aqueous solutions of methanol (10% or 80%).

The laboratory temperature was kept constant at 295 ± 1 K by the laboratory temperature control system.

Parking method experiment

The parking method was initially designed to determine the obstruction factor γ_e of columns packed of nonporous particles in gas chromatography.[17] This method was later used to measure the obstruction coefficient of LC columns.[8,9] It is based on the determination of the band broadening caused by longitudinal diffusion along the column when no flow rate is applied. The longitudinal diffusion coefficient $D_{eff}(v = 0)$ contains the contributions of axial diffusion in the interstitial column volume and of diffusivity across the particle's volume when the particles are porous.

Samples of 5 μL of solution were injected at the desired flow rate (the choice of which depends on the retention factor k' of the sample). Elution is performed during the time necessary for the band to reach about half the column length. The flow is then abruptly stopped and the sample let free to diffuse along the column bed during a certain parking time. Three or four different parking times (e.g., 1, 60, 180, 240, or 480 min) were used. Finally, the mobile phase stream is resumed and the peak profiles are recorded. The slope of a plot of the peak variance vs. the parking time is proportional to the effective axial dispersion coefficient $D_{eff}(v = 0)$ along the column[8] (see discussion later).

Pore-blocking experiment

To measure the external porosity of packed or monolithic columns, it is convenient to block the mesopores of the adsorbent and prevent their access to both eluent and probe compound. This method has the advantage of providing more precise results than the conventional inverse size-exclusion chromatographic experiments, at the cost of the long equilibration time necessary before being able to perform measurements having a relative standard deviation less than 0.2%.[10]

The column was initially rinsed with 2-propanol for 90 min. at a flow rate of 0.75 mL/min, then flushed with nonane for another 90 min, at the same flow rate. The column is then removed from the HP1090 instrument, which was successively purged with 30 mL of 2-propanol and 30 mL of a pure aqueous solution of a phosphate buffer (pH = 2.9), at a flow rate of 4 mL/min. This step is needed to eliminate all nonane from the instrument tubings. Finally, the column is reinstalled in the instrument and the nonane present in the interstitial void volume of the column expelled by flushing the column with a stream of the aqueous solution of the phosphate buffer, at 1.8 mL/min, until the baseline of the detector is noiseless and the first moments of successive injections of dilute NO_3^- are reproducible. This step required about 350 min or 630 mL of aqueous solution, which represents nearly 700 interstitial column volumes.

The total pore blocking method gives excellent results as long as the mobile phase used is pure water and the flow rate applied in the HETP experiments remains smaller than that set to flush out the excess of *n*-nonane in the interstitial volume.[18] Accordingly, the maximum flow rate used in the HETP experiments was 2.5 mL/min.

Results and Discussion

In the following sections, we describe the determinations of the characteristic parameters of the column efficiency, the classical B term of the van Deemter equation (proportional to $2D_{eff}$ or effective bed dispersion coefficient), the effective particle diffusivity, D_p, the solid-liquid overall mass transfer resistance coefficient ($C_h = C_p + C_f$), the eddy dispersion term ($h_{eddy} = \frac{A}{d_p}$), and the film mass transfer coefficient k_f. The molecular diffusivity of the compound considered in the bulk phase was estimated from the Wilke and Chang equation, which is accurate within ~10% in most cases but less than 5% for water-rich eluents.[15]

Determination of the effective axial dispersion along the column

The first term in the right-hand-side of Eq. 1 accounts for the effective axial dispersion along the column. This contribution to band broadening results of the combination of two

diffusion processes that take place respectively in the interparticle space (i.e., in the stream of the mobile phase eluent percolating the bed, volume fraction $\varepsilon_e = 0.364$, molecular diffusivity, D_m) and inside the particles (the porous particles are filled of stagnant eluent, volume fraction $1 - \varepsilon_e = 0.636$, effective particle diffusivity D_p). The effective overall longitudinal diffusion coefficient along the column was measured at a zero flow rate. It is provided by the results of the peak parking experiments.

Figure 1A shows the results of the peak parking experiments for thiourea when the pores of Gemini-C_{18} are accessible and when they are blocked with nonane. When the mesopores were blocked, the mobile phase was pure water buffered at pH = 2.9 with 5 mM phosphate buffer. No methanol was added to this mobile phase because it could have been slightly dissolved in nonane and create an unstable liquid–liquid interface between water and nonane; when the mesopores were not blocked, this mobile phase was diluted with 10% methanol. A minimum of 5% methanol is required in order to avoid pore dewetting. Still, the concentration of methanol is kept small in order to compare pore-blocking and pore accessible experiments. The plots represent the time variance, σ_t^2, of the eluted peaks of thiourea as a function of the parking time (maximum 480 min). The slope of the best line that runs through the experimental data points is proportional to the effective column diffusion coefficient $D_{eff}(v = 0)$[8]:

$$\frac{d\sigma_t^2}{dt} = \frac{2D_{eff}(v=0)}{u_R^2} \tag{13}$$

where u_R is the linear velocity of the compound along the column:

$$u_R = \frac{F_v}{\varepsilon_t \pi r_c^2 (1 + k')} \tag{14}$$

where F_v is the flow rate, r_c the column tube radius (0.23 cm), and k' the retention factor of thiourea ($k' \simeq 0$ when the pores are blocked because thiourea in insoluble in nonane).

The molecular diffusivities of thiourea in pure water and in 90% pure water are 1.10×10^{-5} and 8.78×10^{-6} cm^2/s, respectively. This difference is mostly due to the difference in the eluent viscosities (+25%). The addition of 10% (v/v) methanol to water was necessary to avoid pore dewetting since pure water does not wet C_{18} surfaces under atmospheric pressure, the pressure that prevails along the column during the peak parking method (zero flow rate). Surface tension forces combine with adsorption of gases from the eluent and allow the mesopores to empty. If water would contain no dissolved gas at all, the mesopores might remain filled. When the mesopores are blocked by nonane, the solutes cannot enter into them nor diffuse across the adsorbent particles. Their effective diffusion along the packed bed can take place only in the eluent percolating through the interstitial void, through tortuous paths. The obstruction factor γ_e should be introduced into the expression of $D_{eff}(v = 0)$, because the molecules are constrained to diffuse around the packed solid spheres. Accordingly,

$$D_{eff}(v = 0) = D_{eff} = \gamma_e D_m \tag{15}$$

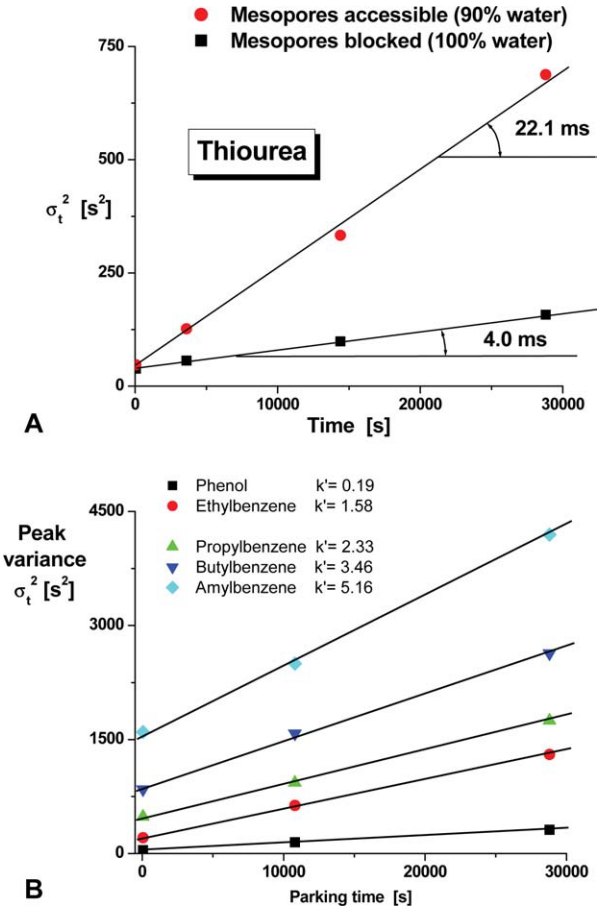

Figure 1. A: Results of the peak parking experiments. Plots of the time variance σ_t^2 of thiourea vs. the parking time in the Gemini-C_{18} column when the mesopores of the particles were blocked by nonane (full squares) or accessible (full circles).

The flow rate used to place the sample zone at half the length of the column was 0.20 mL/min. T = 295 K. Note the restricted effective diffusion of the sample when the pores are blocked, due to both the absence of diffusion inside the particles and the obstruction caused by the impermeable spherical adsorbent. B: Same as in (A) except the mobile phase composition (80% methanol), the samples, and T = 294 K. The flow rate used to place the sample zone in the column was 0.25 mL/min. Note the correlation between the retention factor and the effective axial diffusion along the column, due to enhanced surface diffusion inside the particles. [Color figure can be viewed in the online issue, which is available at wileyonlinelibrary.com.]

When the sample cannot diffuse through the particles, D_{eff} is independent of the linear velocity. We measured from the parking experiments $D_{eff} = 6.12 \times 10^{-6}$ cm^2/s. Given the molecular diffusivities calculated with the Wilke and Chang equation, these measurements give a value of γ_e =0.57, typical for columns packed with spherical particles. McLaren[17] measured an obstruction factor of 0.57 for packed beds with an external porosity close to 0.35. The external porosity of the columns was derived from the variation of the first moment of thiourea with increasing flow rate from 0.1 mL/min (pressure 10 bar) to 2.5 (pressure 280 bar). Figure 2A shows how the external porosity ε_e of Gemini-C_{18} increases with increasing flow rate. This was expected because the

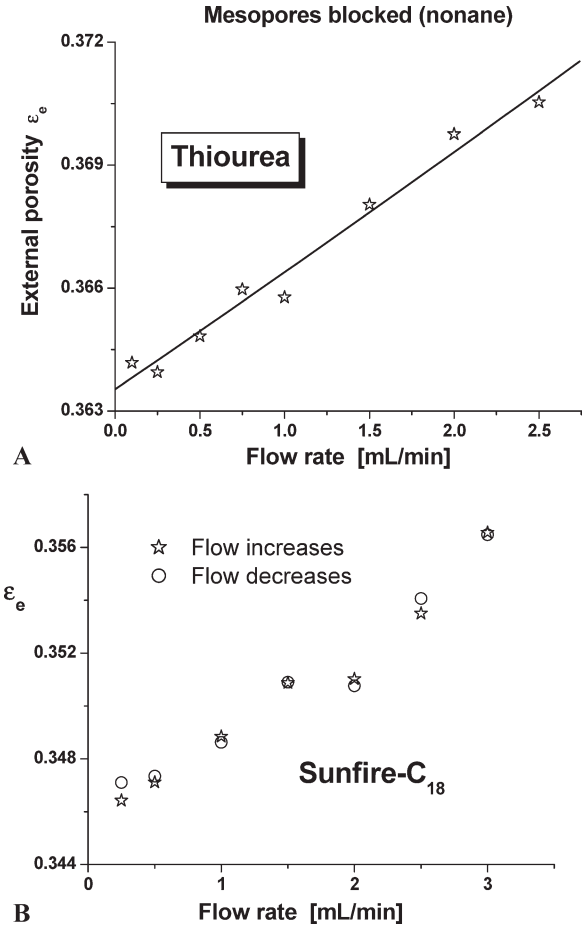

Figure 2. Measurement of the external porosity of the Gemini-C_{18} (A) and Sunfire-C_{18} (B) columns after total blocking of the mesopores by nonane as a function of the fow rate applied.

The decrease of the external porosity as the flow rate decreases is due to expansion of nonane and C_{18}-bonded chains inside the mesopores.

nonane contained in the pores contracts with increasing average column pressure. It is equal to 0.364 under atmospheric pressure and to 0.371 under 280 bar. The compressibility of nonane is 1.2×10^{-4} bar^{-1} at room temperature. When the average column pressure decreases by ca. 140 bar, the relative volume of nonane trapped inside the mesopore volume (771 μL) should increase by 1.7%, e.g., by 13 μL. The experimental results showed that the external volume accessible to water decreases from 923 to 907 μL (-16 μL), which matches well the expansion volume of nonane, given that the C_{18} bonded chains also expand during decompression. The same data are also reported in Figure 2B with the Sunfire-C_{18} column. In these experiments, the measurements were repeated by increasing first and then decreasing the flow rate (from 0.25 mL/min to 3 mL/min). The column packed of particles filled with nonane and eluted by a stream of water circulating between them remains mechanically stable and the measurement of the peak broadening is well reproducible during all chromatographic measurements (see results later).

When nonane is removed from the mesopores, thiourea has full access to the mesopore volume. If we assume that the effective diffusion coefficient is simply the sum of the bulk diffusion coefficient and the particle diffusivity weighed by the volume fractions occupied by the two phases (independent parallel diffusion model), the effective longitudinal diffusion coefficient along the whole column in the immobile liquid phase (i.e., at zero linear velocity) is written[8]:

$$D_{\text{eff}}(v=0) = \frac{\varepsilon_e \gamma_e D_m + (1-\varepsilon_e) D_p}{\varepsilon_t + (1-\varepsilon_t) K} \tag{16}$$

The measurement of D_{eff} in this case gives 7.62×10^{-6} cm^2/s, larger by 25% than the value found when the pores were blocked (i.e., 6.12×10^{-6} cm^2/s). This shows that diffusion in the volume fraction inside the particles (+50%, as $(1-\varepsilon_e)\varepsilon_p = 0.309$ and $1-\varepsilon_e = 0.636$) is slower than in the bulk diffusion medium. This is consistent with sample diffusion through the mesopores network being restricted due to the tortuosity, constriction, and geometrical hindrance that they impose.

The particle diffusivity D_p can be estimated from Eq. 16 with $\gamma_e = 0.57$. Because surface diffusion is zero for non adsorbed sample, we expect D_p to be smaller than the bulk diffusion coefficient for the three reasons given above. The Henry's constant K is equal to 0.278 and $D_p = 6.29 \times 10^{-6}$ cm^2/s ($\Omega = 0.72$), a value clearly smaller than the bulk diffusion coefficient ($D_m = 8.78 \times 10^{-6}$ cm^2/s). In another experiment, phenol was used instead of thiourea. The retention factor of phenol is 10.0 and its diffusion coefficient is nearly 20% smaller than that of thiourea ($D_m = 7.36 \times 10^{-6}$ cm^2/s). Yet, particle diffusivity increases significantly, to $D_p = 1.27 \times 10^{-5}$ cm^2/s ($\Omega = 1.72$). The reason for this increase of Ω is that phenol can diffuse along the mesopore walls, by surface diffusion, a result that is well known in reversed-phase liquid chromatography.[19]

We repeated the same experiments with a methanol/water 80:20 mobile phase, which has a viscosity close to that of the 10:90 methanol/water solution used above (its viscosity is $\simeq$1.27 cP). Measurements were made with phenol, ethylbenzene, propylbenzene, butylbenzene, and amylbenzene. Figure 1B shows the results of the peak parking experiments. The values of D_m, D_{eff}, and D_p are listed in Table 1. As the retention factor increases from ethylbenzene to amylbenzene, Ω increases regularly from 1.12 to 1.78, providing estimates of the contribution of pore diffusivity D_{pores} through[11]:

$$D_{\text{pores}} = \frac{\varepsilon_p}{\tau_p^2} F(\lambda_m) D_m = \Omega_p D_m \tag{17}$$

where ε_p is the particle porosity ($\varepsilon_p = 0.486$ for Gemini-C_{18}). The tortuosity of the mesopore network is related to the porosity of the particles. $\tau_p \simeq 1.3$[8] when the particle porosity is close to 0.50. $F(\lambda_m)$ was estimated from the Brenner and Gaydos correlation[20]:

$$F(\lambda_m) = 1 + \frac{9}{8}\lambda_m \ln \lambda_m - 1.54\lambda_m \tag{18}$$

where λ_m is the ratio of the solute molecular radius to the pore radius. The former radius was calculated from the molar

Table 1. List of Samples

Sample	V_b (cm^3/mol)	Eluent (% water)	T (K)	D_m (cm^2/s)	k'	Ω	Ω_s	h_{eddy}	C	k_f (cm/s)	k_f Wilson & Geankoplis (cm/s)	k_f Kataoka (cm/s)
Thiourea	77.0	100% + 5 Mm phosphate	295	1.10 E−05	0.000	0	0	17	0	–	–	–
Thiourea	77.0	90% + 5 mM phosphate	295	8.78 E−06	0.135	0.47	0.27	4.7	0.045	0.027	0.113	0.084
Phenol	103.4	90% + 5 mM phosphate	295	7.36 E−06	10.00	1.47	1.28	7.4	0.099	0.029	0.094	0.070
Phenol	103.4	20%	294	7.79 E−06	0.200	0.31	0.11	5.3	0.070	0.017	0.100	0.074
Ethyl-benzene	140.4	20%	294	6.48 E−06	1.580	0.88	0.69	5.6	0.052	0.040	0.083	0.062
Propyl-benzene	162.6	20%	294	5.94 E−06	2.330	1.07	0.88	7.2	0.066	0.030	0.076	0.057
Butyl-benzene	184.8	20%	294	5.50 E−06	3.460	1.28	1.10	7.8	0.065	0.030	0.071	0.052
Amyl-benzene	207.0	20%	294	5.14 E−06	5.160	1.54	1.36	7.5	0.072	0.026	0.066	0.049

Molar Volumes at the Boiling Point (V_b), Eluents, Temperatures (T), Bulk Diffusion Coefficients (D_m), Retention Factors (k'), relative particle diffusivity to bulk diffusion (Ω), relative surface diffusion to bulk diffusion (Ω_s), limiting eddy dispersion term (h_{eddy}), total solid–liquid mass transfer coefficient (C), film mass transfer coefficients (k_f) from experiments and available correlation in the literature (Wilson and Geankoplis, Kataoka).

volume of the sample (V_b), assuming a spherical shape (see Table 1). The average pore size radius after derivatization of the Gemini material is 90 Å. The values of Ω_p in Eq. 17 can be estimated for all the solutes as well as the contribution $\Omega_s = \Omega - \Omega_p$ of surface diffusion. Figure 3 summarizes these results. According to Eq. 17, the equivalent diffusion inside the mesopores referred to the whole particle volume is close to 80% slower than the bulk molecular diffusion coefficient D_m for all the phenyl derivatives. Normalized to the pore volume, only, pore diffusion is about 40% slower than bulk diffusion. The contribution of surface diffusion increases linearly at low retention factors (it is controlled by the surface concentration, which increases with increasing retention factor), reaches a maximum, and finally decreases when adsorption becomes strong (surface diffusion is then controlled by the isosteric heat of adsorption Q_{st}). A model of surface diffusion previously derived can be tested by measuring the ratio of the frequency factors $\frac{D_{S,0}}{D_{m,0}} \simeq 1$ for unretained compounds when k' tends toward zero (and the isosteric heat of adsorption Q_{st} goes to zero) from the initial slope of the graph shown in Figure 3. This model of surface diffusion is written[11]:

$$\Omega_s = 2\frac{\varepsilon_p}{\tau_p^2}\frac{\alpha}{r_p}\frac{\varepsilon_t}{1-\varepsilon_t}k'\frac{D_{S,0}}{D_{m,0}}\exp\frac{\beta Q_{st}}{RT} \tag{19}$$

When k' tends toward zero, so does Q_{st} and $D_{s,0}$ should theoretically tend toward $D_{m,0}$, which we need to check. We derive from Eq. 19 that:

$$\lim_{k'\to 0}\frac{\Omega_s}{k'} = 2\frac{\varepsilon_p}{\tau_p^2}\frac{\alpha}{r_p}\frac{\varepsilon_t}{1-\varepsilon_t} \tag{20}$$

where $\alpha = 1/\rho_{BP}\%_{Matrix}S_p$[11] is a structural parameter which depends on the density of the bonded phase material (ρ_{BP} = 1.7 g/cm^3), the mass fraction percent of underivatized packing material ($\%_{Matrix} = 85\%$), and the specific surface area of this material (S_p = 375 m^2/g). r_p is the average pore size of the derivatized packing material (90 Å). Hence, $\alpha/r_p = 0.37$. ε_p = 0.486, τ_p = 1.3, and ε_t = 0.673. The best value of the initial slope of the plot of Ω_s vs. k' in Figure 3 is 0.61. From Eq. 20, we found that the limit of the ratio $D_{S,0}/D_{m,0}$ is equal to 0.76, a value sufficiently close to 1 to confirm the validity of the diffusion model Eq. 19.

In conclusion of this section, the peak parking method provides estimates of the axial dispersion term and of the particle diffusivity D_p of small molecules. These diffusion coefficients will be used later to estimate the mass transfer resistance contributions of the slow restricted diffusion across particles (third term in the right-hand-side of Eq. 1).

Determination of the eddy dispersion term

As the flow rate is increased and the reduced linear velocity becomes larger than one, the longitudinal diffusion term in Eq. 1 reduces to the external diffusion term $\gamma_e D_m$ because the convection of the mobile phase causes the concentration of the solute around each particle to become the same at a rate faster than diffusive transfer can take place across particles in the axial direction of the column. Then, the solute concentration profiles around and inside each individual particle have radial symmetry. The particles do not participate to overall longitudinal diffusion of the solute since the net diffusive flux across any one of them is zero. The value of γ_e was measured to be 0.57 in the previous section, using the peak parking method.

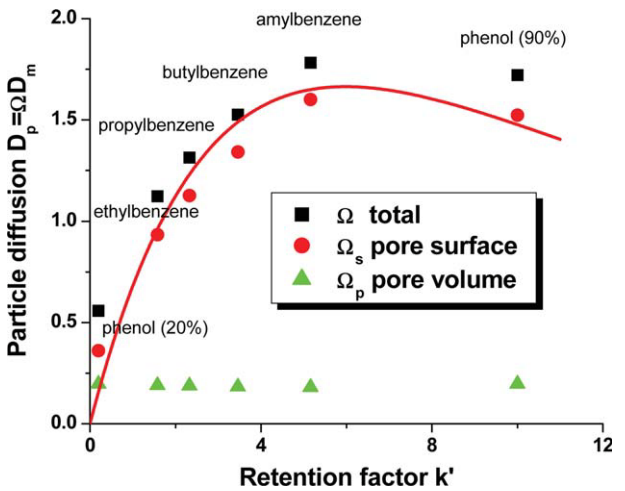

Figure 3. Contributions of the pore volume (Ω_p) and the pore surface (Ω_s) to the overall particle diffusivity Ω measured from the peak parking method for different small molecules with different retention factors.

The solid line is the best fitting of the experimental data to the surface diffusion model given in Eq. 19. [Color figure can be viewed in the online issue, which is available at wileyonlinelibrary.com.]

When the mesopores are blocked by nonane, the film mass transfer resistance can be neglected because there are no concentration gradient at the interface between the nonane-filled pores and the water stream. The retention factor of thiourea is zero when the pores are blocked because thiourea is not soluble in nonane and its adsorption on the external surface of the particles is negligible. Thus, no diffusion takes place inside the mesopores nor from the percolating mobile phase to the mesopores nor vice versa. Accordingly, the last two terms in Eq. 1 vanish and a plot of the reduced column efficiency vs. the reduced velocity gives h_{eddy}. This term is the sum of the first two terms in Eq. 1 as it includes the contribution of the net longitudinal diffusion of thiourea in the interstitial void. Accordingly, the total reduced HETP term is written:

$$h = \frac{2\gamma_e}{v} + h_{\text{eddy}} \tag{21}$$

Figure 4 shows the peaks of thiourea eluted from the column (Figure 4A) and from a zero-volume union connector. These two chromatograms were recorded at the same flow rate of 0.75 mL/min ($v \simeq 10$). The peak eluted from the column is slightly fronting (this is seen more clearly in Figure 4C, recorded under different conditions, as explained later). Injection of a dilute aqueous solution of sodium nitrate gives a peak exhibiting the same fronting, which confirms that the origin of this anomaly is probably in some slight radial heterogeneity of the packed bed. It certainly cannot come from any specific interactions between the analyte and the external surface of the particles, on which it is not retained. This results in a value of the A term that is large compared to the one expected from a well–packed columns (in which $A \simeq 1$ to 3).

This value of the A-term, measured with the mesopores blocked by nonane, permits the determination of the amplitude of the velocity inequality across the column and the corresponding flow and diffusion characteristic distances separating one velocity extreme from the other, parameters identified by Giddings.[1] The first moments (μ_1 and $\mu_{1,ex}$) and the second central moments (μ'_2 and $\mu'_{2,ex}$) were calculated from the recorded peaks, according to Eqs. 9, and h_{eddy} was derived from Eq. 21.

Figure 5A shows the plot of the reduced HETP term h_{eddy} vs. the reduced velocity. The limiting value reached at high reduced linear velocities ($v > 15$) is of the order of 17, a value much larger than the one expected for well packed columns (usually between 1 and 3). The large value of the reduced A term of the Gemini-C_{18} column is directly related to the peak fronting at its base. As a consequence, an additional source of velocity inequality must probably be included in the general eddy dispersion model applied to this problem.

Peak fronting can be caused by transcolumn flow heterogeneity[21] with the mobile phase velocity being lower in the central than in the wall regions. A radial distribution of the mobile phase velocity is due to packing heterogeneity, arising during the preparation of the column. A qualitative description of the origin of peak fronting can be proposed. Let assume that the sample distribution at column inlet is planar but that the flow pattern across the column is parabolic, the eluent flowing faster close to the column wall than in its center, and that there is no other source of band broad-

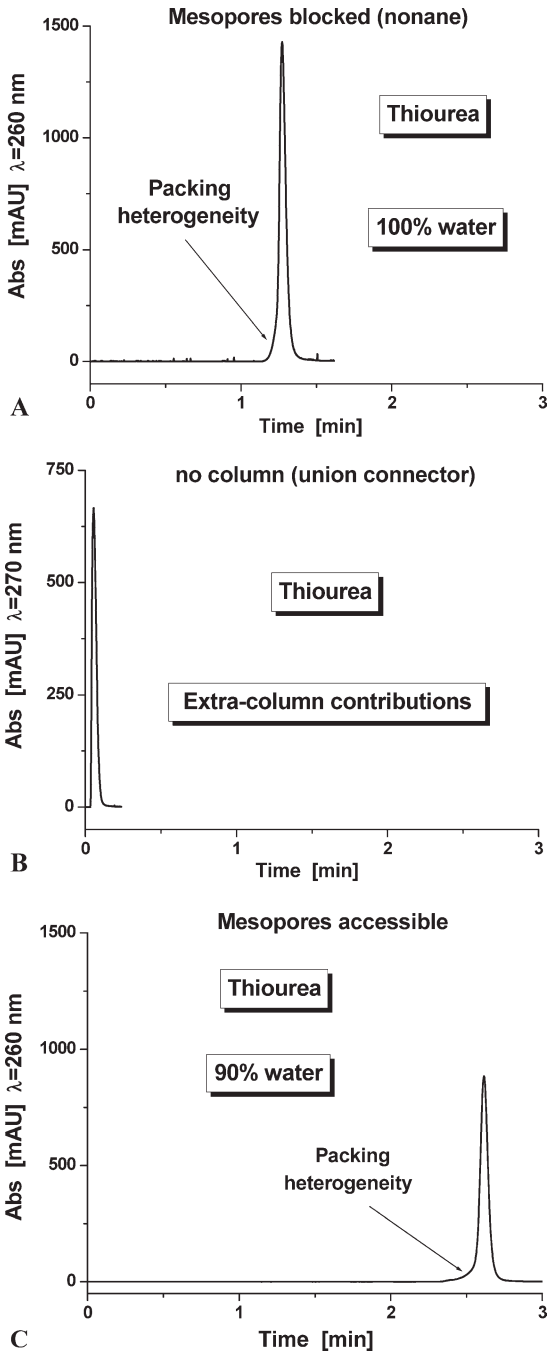

Figure 4. A: Peak profile of thiourea recorded when the mesopores were blocked by nonane after the total pore blocking experiments.

Column: Gemini-C_{18} (150 × 4.6 mm). $T = 295$ K. Flow rate: 0.75 mL/min. Mobile phase: pure water with 5 mM phosphate buffer at pH = 2.9. Note the slight fronting at the base of the peak. Strictly similar fronting was observed with injection of sodium nitrate (B) Same as in (A) except the column was removed from the chromatograph and replaced with a union connector. C: Same as in Figure (A) except the mesopores were accessible after removal of nonane in the mesopores and using a mobile phase containing 10% methanol in volume.

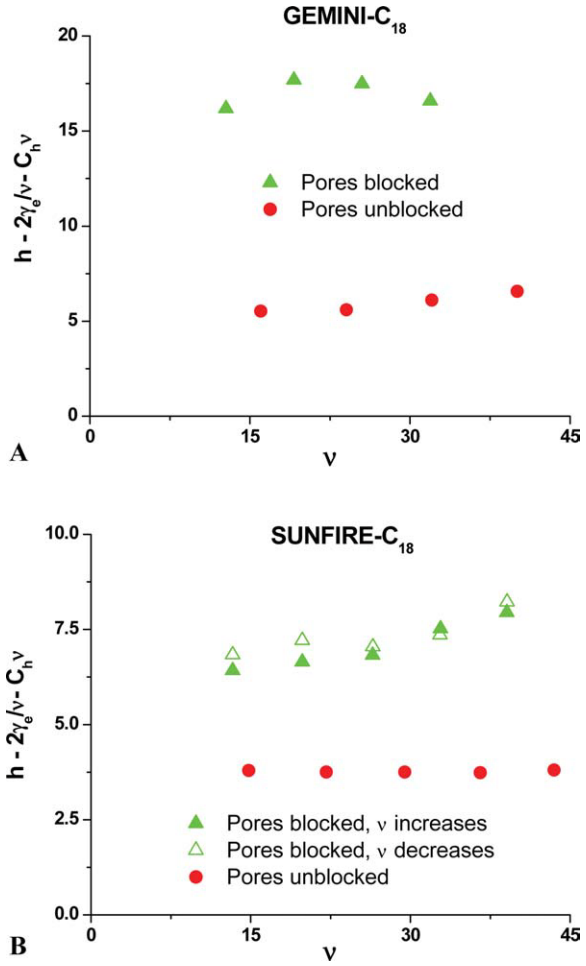

Figure 5. A: Plot of the reduced eddy dispersion term alone measured with thiourea before and after total blocking of the mesopores of the Gemini-C_{18} column with nonane.

Same experimental conditions as in Figure 4A and 4C. B: Same figure with the column Sunfire-C_{18}. In both cases, the A-term is much smaller when the sample can diffuse through the particles. [Color figure can be viewed in the online issue, which is available at wileyonlinelibrary.com.]

ening than this radial flow heterogeneity across the packed column. The chromatogram at the column outlet ($z = L$) can be calculated. Let $x = \frac{r}{R}$ be the dimensionless radial coordinate. The linear velocity $u(x)$ of the eluent at the radial coordinate x is written:

$$u(x) = u(0)\left[1 + \omega_{\beta,c}x^2\right] \tag{22}$$

with $\omega_{\beta,c} > 0$ for peak fronting.

Let assume a dispersionless column (ideal chromatography) in order to calculate only the effect of the velocity gradients from the center to the wall of the column. This assumption can be checked based on an estimate of the radial dispersion coefficient of thiourea, D_r, in a packed bed of nonporous particles (Gritti et al., in press):

$$D_r = \varepsilon_e\gamma_e D_m + \gamma_r\frac{1}{2}ud_p \tag{23}$$

The value of γ_r is close to 0.30 for columns packed with 5 μm particles.[22] $\varepsilon_e = 0.364$, $\gamma_e = 0.57$, $D_m = 1.10 \times 10^{-5}$ cm^2/s, $d_p = 5\mu m$, and the minimum and maximum values of the superficial linear velocity are $u_{min} = 0.027$ cm/s (0.1 mL/min) and $u_{max} = 0.68$ cm/s (2.5 mL/min), respectively. The maximum value of D_r is then 5.3×10^{-5} cm^2/s. At this high linear velocity, the mean elution time of thiourea is about $t_{R,min} = 22$ seconds. The average radial displacement probed by thiourea is $\sqrt{2D_r t_R} = 0.048$ cm, a distance of about 20% of the column radius (0.230 cm). The minimum value of D_r is 4.3×10^{-6} cm^2/s and the residence time is 545 s. The average radial diffusion distance is now equal to 0.068 cm, a value still smaller than the column radius (30%). Clearly, transcolumn effects are essentially governed by the radial flow pattern at high reduced linear velocities.

Assuming a cylindrical symmetry, the ideal normalized chromatogram $C(t)$ is written:

$$C(t) = 2\int_0^1 \delta\left(t - \frac{L}{u(x)}\right)xdx \tag{24}$$

where $\delta(t)$ is the Dirac pulse function.

The first and second central moments of this concentration distribution are:

$$\mu_1 = \left[\frac{L}{u(0)}\right]\frac{\ln(1+\omega_{\beta,c})}{\omega_{\beta,c}} \tag{25}$$

$$\mu_2' = \left[\frac{L}{u(0)}\right]^2\left[\frac{1}{\omega_{\beta,c}+1} - \frac{\ln^2(1+\omega_{\beta,c})}{\omega_{\beta,c}^2}\right] \tag{26}$$

When $\omega_{\beta,c}$ is small and tends toward zero, the reduced eddy HETP term associated with the transcolumn effect simplifies to:

$$h_{eddy,transcolumn} = \frac{L}{d_p}\frac{\mu_2'}{(\mu_1)^2} \simeq \frac{L}{d_p}\frac{\omega_{\beta,c}^2}{12} \tag{27}$$

The column length is $L = 15$ cm and the particle size is $d_p = 5$ μm. The additional transcolumn reduced eddy dispersion term of 15 is consistent with an average transcolumn velocity bias $\omega_{\beta,c}$ of 8 %, which is a physically acceptable velocity bias in a poorly packed column over a distance equal to the column internal radius. The slight peak fronting observed can definitely be explained by such transcolumn effects. To match precisely the shape of the peak profiles shown in Figure 4A, the flow pattern would rather be flat in the center of the column and vary more steeply close the wall, which is consistent with experimental determinations.[23]

Figure 4C shows the experimental peak profile of thiourea on the Gemini-C_{18} column at the same flow rate of 0.75 mL/min, but under such conditions that the particle mesopores are accessible. Figure 5A shows the experimental reduced HETP curve. The eddy dispersion term, h_{eddy}, was calculated by subtracting from the experimental h data acquired at high flow rates the contributions of the longitudinal diffusion term $(\frac{2\gamma_e}{\nu})$ and the overall mass transfer resistance between the particles and the mobile phase ($C_h\nu$). The coefficient C_h was

measured from the slope of the h vs. v plot in the high linear velocity domain ($v > 15$):

$$h_{\text{eddy}} = h - \frac{2\gamma_e}{v} - C_h v \tag{28}$$

Surprisingly, the overall eddy dispersion term measured for thiourea is much lower ($h_{\text{eddy}} = 7$) when the mesopores are accessible than when they are blocked by nonane ($h_{\text{eddy}} = 17$). The same column was used in the two series of measurements and the peak fronting observed is due to an excessive degree of radial heterogeneity of the bed, not to any nonlinear effect. This suggests that either the eddy dispersion contribution in columns packed with porous particles is not the same as in columns packed with nonporous particles of the same size and shape or that transparticle diffusion provides an unexpectedly efficient mean of relaxing the consequences of a velocity bias on the radial homogeneity of the band. The average velocity bias, $\omega_{\beta,c}$, of the transcolumn effect is of the order of 4.5%. However, Eq. 27 does not apply strictly in this case because, to some extent, radial dispersion may contribute to relax the radial concentration gradient across the column diameter. So, the new value of the best parameter $\omega_{\beta,c}$ should necessarily be smaller than in the pore blocked case and reveal the more effective radial mixing of the band during its axial migration than in the pore blocked case.

We need to understand why the A-term of a packed column varies in such a large proportion depending on whether the pores of the particles are blocked or not. A first interpretation would be that porous particles allow a better radial homogenization of the band during their elution than nonporous particles. The measurements of the reduced HETP are certainly accurate, due to the use of the moment analysis method rather than that of the far more approximate peak width at half-height method, and sufficiently precise ($\pm$ 10%), as illustrated by the modest scatter of the HETP data points in Figure 7. The pore-blocking method uses pure water as the eluent and the values of the first moments are consistent with the external porosity of the packed bed. Still, this method needs to be validated with other columns which do not exhibit peak fronting.

We repeated the same pore-blocking experiments with a column showing no peak fronting (Sunfire-C_{18}, $L = 15$ cm, $d_p = 5$ μm). The results are shown in Figure 5B. The additional transcolumn reduced eddy dispersion term is about three times smaller (4.5) and the additional transcolumn velocity bias decreases to $\omega_{\beta,c} = 4.2$ %. However, when the pores are unblocked, the reduced eddy dispersion due to the transcolumn effect in the Sunfire column is only of the order of 1.5 e.g. three times smaller than when the mesopores are blocked. The transcolumn velocity bias $\omega_{\beta,c}$ is close to 2.5% which is an acceptable value in a well-packed column.[24] This ratio of three (1.5 vs. 4.5) is the same as the one found for the Gemini column (5 vs. 15). The large A-term values observed with the Gemini columns are simply explained by the presence of the slight peak fronting.

In conclusion, the value of the eddy dispersion term depends on whether the particles are porous or not. Eddy dispersion is smaller with porous particles, probably because radial dispersion is faster across a bed of porous particles than across one of nonporous particles. Porous particles minimize the band broadening effect caused by the transcolumn flow velocity pattern. This result is original and seems to be important for a better understanding of mass transfer kinetics in chromatographic columns. That the radial dispersion coefficient D_r of a compound depends much on whether the pores are blocked or not may explain why we observed high and low A-term values, respectively. However, past investigations on radial dispersion in beds packed with porous and nonporous spheres showed little difference in D_r values because of the extremely low permeability of porous particles.[25] This is surprising because the volume of stagnant eluent inside the porous particles represents about 25% of the empty column tube volume while the interparticle volume accounts for 37%, two very comparable volume fractions. This internal pore volume is far from negligible. The associated internal diffusion process speeds up radial mass transfer across the column. Most importantly, analyte molecules are not constrained to move around the particles in the interstitial volume. They can bypass these lengthy pathways by diffusing through the porous particles. In addition, the presence of the internal volume increases the analyte residence time inside the column, hence contributes to a more effective relaxation of the radial concentration gradient.

Determination of the solid–liquid film mass transfer resistance term

We consider three groups of compounds having different retention factors, thiourea ($k' \simeq 0.15$), phenol ($k' \simeq 10$), and a few moderately retained compounds ($0 < k' < 6$).

Unretained Sample. The measurement of the particle diffusivity of thiourea, D_p, using the peak parking method allows the direct determination of the resistance to mass transfer between the moving and the stationary eluents. We define the coefficient C_p as:

$$C_p = \frac{1}{30}\frac{\varepsilon_e}{1-\varepsilon_e}\left(\frac{\delta_0}{1+\delta_0}\right)^2 \frac{1}{\Omega} v \tag{29}$$

The mobile phase used was methanol/water (10:90, v/v) to avoid pore dewetting (see above). The reduced linear velocity is determined from the molecular diffusivity of thiourea in this new eluent, e.g., $D_m = 8.78 \times 10^{-6}$ cm^2/s. The values of Ω ($D_p = \Omega\ D_m$) estimated from the peak parking method data is 0.72. We found that $\delta_0 = 1.10$ and $\varepsilon_e = 0.364$. Accordingly, C_p is equal to 0.73×10^{-2}. The experimental overall C term is equal to 4.55×10^{-2}. Thus, the transparticle mass transfer resistance plays a minor role in the resistance to mass transfer between the solid particles and the mobile phase (it accounts for ca. 16% of this resistance). The film mass transfer resistance is mostly responsible for the HETP increase at high linear velocity. Accordingly, we define the parameter C_{k_f} as follows

$$C_f = C - C_p = \frac{1}{3}\frac{\varepsilon_e}{1-\varepsilon_e}\left(\frac{\delta_0}{1+\delta_0}\right)^2 \frac{D_m}{k_f d_p} \tag{30}$$

This allows the determination of the average film mass transfer coefficient, k_f, for reduced linear velocities between

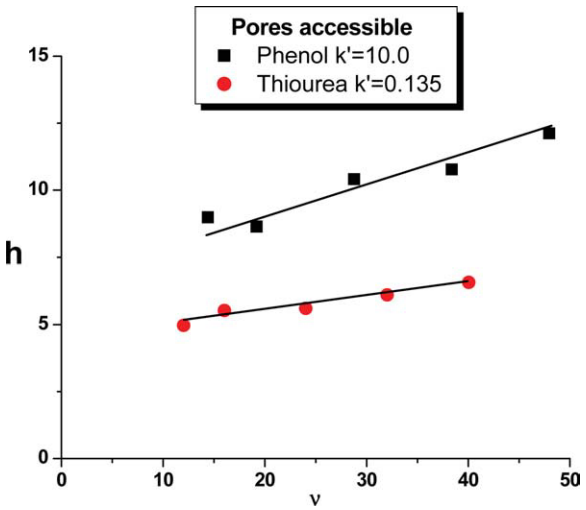

Figure 6. Plot of the total reduced HETP of strongly retained (full squares) and poorly retained (full circles) compounds when the mesopores of the Gemini-C_{18} particles are accessible.

Same experimental conditions as in Figure 4C. Note the larger A-term of phenol ($\simeq$7) compared to that of thiourea ($\simeq$4). [Color figure can be viewed in the online issue, which is available at wileyonlinelibrary.com.]

15 and 40. The experimental constant C was determined by considering the HETPs at the four highest reduced linear velocities (ν =16, 24, 32, and 40) for which the eddy dispersion term has reached its limiting value. $C_f = 3.81 \times 10^{-2}$ and, according to Eq. 30, the average film mass transfer coefficient is $k_f = 0.024$ cm/s.

Strongly Retained Component. Phenol was eluted with the same mobile phase as above (methanol/water, 10:90, v/v). Its molecular diffusivity is $D_m = 7.18 \times 10^{-6}$ cm^2/s and its retention factor about 75 times larger than that of thiourea in this mobile phase ($k'_{phenol} = 10.0$ *vs* $k'_{thiourea} = 0.135$) and $\delta_0 = 19.3$. The peak parking experiment gives a particle diffusivity of phenol $D_p = 1.27 \times 10^{-5}$ cm^2/s. This gives a value of $\Omega = 1.72$, showing that Ω increases with increasing solute retention, because the sample concentration adsorbed onto the adsorbent surface increases (large k' values) and so does the surface diffusion of phenol along the mesopore walls.[19] The value of C_p for this strongly retained solute is 1.00×10^{-2}, just 25% larger than in the case of an unretained compound.

Even for this strongly retained compound, the contribution of the resistance to mass transfer due to finite diffusion through the spherical particles is relatively minor.

Figure 6 compares the reduced HETPs of thiourea and phenol when the pores are totally accessible. The best C term is equal to 9.91×10^{-2}. According to Eq. 30, the average film mass transfer coefficient is $k_f = 0.028$ cm/s, a value in excellent agreement with the value measured for thiourea.

Intermediate Retention Factors. The same strategy was used to measured the film mass transfer coefficients of ethylbenzene, propylbenzene, butylbenzene, and amylbenzene in a 80:20 v/v methanol/water solution (Figure 7). The higher methanol concentration was selected to reduce the retention factors. All the results are listed in Table 1. All the values obtained for k_f are randomly distributed between 0.015 and 0.037 cm/s with an average of 0.027 cm/s.

Comparison with Data from Available Empirical Correlations and from Literature The correlations available in the literature are the empirical Wilson and Geankoplis correlation[5] and the Kataoka[6] correlation. The former is written

$$Sh = \frac{k_f d_p}{D_m} = \frac{1.09}{\varepsilon_e} v_S^{1/3} \tag{31}$$

where v_S is the reduced superficial linear velocity ($v_S = \varepsilon_e v$).

The latter is written:

$$Sh = \frac{k_f d_p}{D_m} = 1.85 \left(\frac{1-\varepsilon_e}{\varepsilon_e}\right)^{1/3} v_S^{1/3} \tag{32}$$

When ν increases from 15 to 40, the average value of $\nu^{1/3}$ is 3. The results of the calculations made with Eqs. 31 and 32 are given in Table 1. The Wilson and Geankoplis correlation gives values of k_f scattered between 0.066 and 0.113 cm/s. The Katakoa correlation provides slightly lower estimates of k_f, which are also significantly scattered, with values between 0.049 and 0.084 cm/s. On the average, these two correlations overestimate the values of the actual film mass transfer coefficient found in this work at high reduced linear velocity by factors 3.5 and 2.5, respectively.

Miyabe et al.[7] recently measured the film mass transfer, k_f, of ethylbenzene on a 18 μm nonporous silica-C_{18} packed column eluted with a mobile phase containing 30% methanol in water, giving $D_m = 5.13 \times 10^{-6}$ cm/s. They found at 298 K and for reduced interstitial linear velocities ν between 36 and 230 (average $\nu^{1/3} = 5$) an average Sherwood number of 8, e.g., an average film mass transfer coefficient k_f equal 0.023 cm/s. This value agrees well with the estimate given by the Kataoka model, while the Wilson and Geankoplis correlation overestimates the experimental value by 30%. This better agreement originates certainly from the fact that these correlations were derived from data measured with nonporous particles as those used by Miyabe.[7]

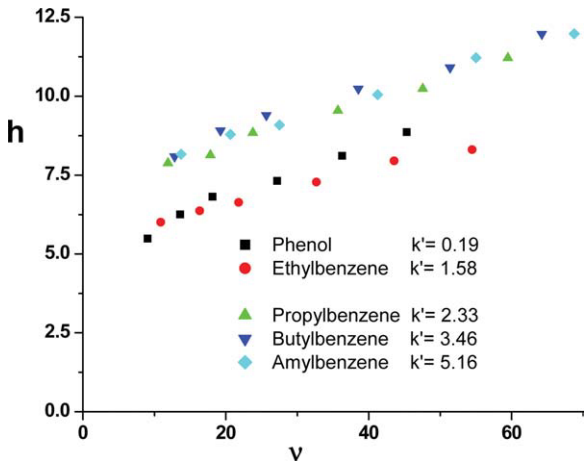

Figure 7. Same as in Figure 6 except the mobile phase composition, 80% methanol, different retained samples, and T = 294 K.

[Color figure can be viewed in the online issue, which is available at wileyonlinelibrary.com.]

It was also experimentally reported that k_f decreases with decreasing average particle size when the measurements are made in a similar range of linear velocities. This is related to the fact that k_f is inversely proportional to the power two third of the average particle diameter. Hong et al.[26] measured decreasing values of k_f from 0.200, to 0.162, 0.101, 0.081, and to 0.038 cm/s as the average particle size increased from 3.74 (average $v^{1/3} = 2.34$), to 5.21 (average $v^{1/3} = 3.17$), 10.6 (average $v^{1/3} = 4.01$), 14.92 (average $v^{1/3} = 4.50$), to 47.1 μm (average $v^{1/3} = 7.62$) when using propylbenzene as the solute and an aqueous mobile phase containing 70% methanol. These experimental values of k_f are much larger than those estimated from the Wilson and Geankoplis or the Kataoka correlations by factors of 2 and 3, respectively. Our results are not consistent with these data since we measured k_f values smaller than those predicted by the correlations. The difference could be explained by a wrong estimate of the particle diffusivity, D_p, a parameter difficult to estimate when peak parking experiments are not carried out. This means that Hong et al. underestimated the surface diffusion contribution, which is consistent with the values of $\Omega_s/\Omega_p = 1.1$ which they reported for propylbenzene. Based on the results of the peak parking method, we found this ratio to be 6.0 for propylbenzene.

In conclusion, the accurate determination of the coefficient k_f requires the measurement of the column effective diffusivity D_{eff} and the peak parking method is the most accurate method for this purpose. The value obtained for k_f will likely be smaller for porous than for nonporous particles because only the fraction $1 - \varepsilon_p$ of the external surface area of the particle is a solid surface. The local concentration gradients are large only at the liquid–solid interface wall of the particles, while the concentration gradients are smoother at the liquid–liquid interface between the throughpores and the external eluent.

Conclusions

We proposed and applied an original protocol for the experimental determination of the parameters of each one of the individual contribution to the overall mass transfer kinetics of analytes in HPLC columns.

(1) The peak parking method yields the effective diffusivity, D_{eff}, of solutes in a bed of porous particles. It provides accurate and precise estimates of the particle diffusivity (D_p) and of the contribution to mass transfer resistance of the diffusion of the analyte inside porous particles (C_p).

(2) The pore blocking experiments combined with the peak parking method permits the determination of the obstruction factor of the column bed (γ_e).

(3) The limiting eddy dispersion term is obtained by subtracting the contribution of the reduced HETP ($C_h v$) from the overall HETP (h) at reduced linear velocities larger than 15. The study and the qualitative evaluation of the degree of transcolumn flow heterogeneity is made possible.

(4) The film mass transfer coefficient k_f is unambiguously determined as the difference between the C_h and C_p terms, within a limited domain of reduced linear velocities ($2.5 < v^{1/3} < 3.5$).

The measurements of these parameters of the mass transfer kinetic in a chromatographic column gave three important new insights to the theory of mass transfer in HPLC columns.

(1) Unexpectedly, eddy dispersion taking place in beds packed with nonporous particles is not equivalent to that observed for beds of porous particles of the same size. Eddy dispersion is much less when the eluent may diffuse through the porous particles. Thus, a new theory of eddy dispersion is needed that would take into account the role played by particle diffusivity in the exchange mechanism between streamlines of the mobile phase having different velocities from the center to the wall of the column.

(2) The film mass transfer resistance between particles and mobile phase controls the overall C_h term. Its relative contribution increases with increasing retention factor because surface diffusion speeds up mass transfers across particles and the concentration gradient of adsorbate increases with increasing retention factor. Based on the work of Miyabe et al.[7] and on the present work, we conclude that the apparent film mass transfer resistance is nearly twice smaller with porous than with nonporous particles. This ratio is most certainly related to the particle porosity ($\varepsilon_p \simeq 0.5$).

(3) Our results validate a model of surface diffusion[11] which takes into account the average pore size of the mesopores, the specific surface area of the packing material, and the particle tortuosity factor.

Further work will consist in studying the mass transfer kinetics of various compounds in columns packed of nonporous particles of sizes in between 2 and 5 μm, the conventional range of particles used to packed current HPLC columns and comparing the results (axial diffusion, eddy dispersion, and film mass transfer) with those obtained for conventional porous materials. The total pore blocking method has not been frequently used yet and its validation might require more experimental data. This will help in establishing a new model of eddy dispersion in packed columns and in better predicting the relationships between column efficiency and column structure. The effect of the average pore size of the particles on the column efficiency are worth studying carefully because they affect the diffusion mechanism of large molecules such as proteins, hence their eddy dispersion term, much more than those of low molecular weight solutes.

The same experimental approach will be applied to the study of the kinetic phenomena that control the mass transfer kinetics in monolithic columns, for which a relatively large A-term limits the performance.

Acknowledgments

This work was supported in part by grant CHE-06-08659 of the National Science Foundation and by the cooperative agreement between the University of Tennessee and the Oak Ridge National Laboratory.

Notation

Roman letters

A = eddy dispersion coefficient (m^2)
C = sample mobile phase concentration (kg/m^3)
C_h = overall solid–liquid mass transfer coefficient
C_f = film solid–liquid mass transfer coefficient
C_p = transparticle solid–liquid mass transfer coefficient
D_{pores} = mesopore diffusion coefficient (m^2/s)
D_{eff} = axial diffusion coefficient of the column (m^2/s)
d_p = average particle size (m)
D_p = particle diffusivity (m^2/s)

$D_{m,0}$ = frequency factor of bulk diffusion (m^2/s)
D_m = bulk molecular diffusion coefficient (m^2/s)
$D_{S,0}$ = frequency factor of surface diffusion (m^2/s)
$F(\lambda_m)$ = pore steric hindrance parameter
F_v = flow rate (m^3/s)
h = total reduced column HETP
h_{eddy} = reduced eddy dispersion HETP
k' = retention factor
K = Henry's constant
k_f = film mass transfer coefficient (m/s)
L = column length (m)
M = molecular weight (g/mol)
Q_{st} = isosteric heat of adsorption (J/mol)
r_c = internal column tube radius (m)
R = ideal gas constant (J/mol/K)
r_p = average pore radius in volume (m)
Sh = Sherwood number
S_p = specific surface of the solid matrix before derivatization (m^2/kg)
t = time variable (s)
T = temperature (K)
u = interstitial linear velocity (m/s)
u_R = sample migration linear velocity (m/s)
u_S = superficial linear velocity (m/s)
V_0 = hold-up volume of the column (m^3)
V_R = elution volume of the retained sample (m^3)
V_b = molar volume of the sample at its boiling point (m^3/mol)
x = molar fraction

Greek letters

α = structural parameter defined in Eq. 19
β = coefficient defined in Eq. 19
η = eluent's viscosity (Pa.s)
δ_0 = retention parameter defined in Eq. 5 (s)
ε_e = external column porosity
ε_p = particle porosity
ε_t = total column porosity
ϕ = associative factor of pure eluent
γ_e = external obstructive factor with nonporous particles
γ_r = radial obstruction coefficient in Eq. 23
λ_m = analyte to pore size ratio
μ_1 = first moment (s)
$\mu_{1,ex}$ = first moment of the extra-column band profiles (s)
μ'_2 = second central moment (s^2)
$\mu'_{2,ex}$ = second central moment of the extra-column band profiles (s^2)
v = reduced interstitial linear velocity (m/s)
v_S = reduced superficial linear velocity (m/s)
$\omega_{\beta,c}$ = transcolumn relative velocity inequality for a parabolic flow pattern
Ω = ratio of the particle diffusivity to the bulk diffusion coefficient
Ω_p = ratio of mesopore diffusion to the particle diffusivity
Ω_s = ratio of surface diffusion to the particle diffusivity
ρ_{BP} = packing material density (kg/m^3)
σ_t = time peak standard variance (s)
τ_p = particle tortuosity factor

Literature Cited

1. Giddings J. *Dynamics of Chromatography*. New York, NY: Marcel Dekker, 1965.
2. Guiochon G, Felinger A, Katti A, Shirazi D. *Fundamentals of Preparative and Nonlinear Chromatography*, 2nd ed. Boston, MA: Academic Press, 2006.
3. Kucera E. Contribution to the theory of chromatography. Linear non-equilibrium elution chromatography. *J Chromatogr*. 1965;19: 237–258.
4. Miyabe K. Evaluation of chromatographic performance of various packing materials having different structural characteristics as stationary phase for fast high performance liquid chromatography by new moment equations. *J Chromatogr A*. 2008;1183:49–64.
5. Wilson E, Geankoplis C. Liquid mass transfer at very low Reynolds number in packed beds. *J Ind Eng Chem (Fundam)*. 1966;5:9–14.
6. Kataoka T, Yoshida H, Ueyama K. Mass transfer in laminar region between liquid and packing material surface in the packed bed. *J Chem Eng Jpn*. 1972;5:132–136.
7. Miyabe K, Ando M, Ando G N Guiochon. External mass transfer in high performance liquid chromatography systems. *J Chromatogr A*. 2008;1210:60–67.
8. Gritti F, Guiochon G. Effect of the surface coverage of C $_{18}$-bonded silica particles on the obstructive factor and intraparticle diffusion mechanism. *Chem Eng Sci*. 2006;61:7636–7650.
9. Miyabe K, Matsumoto Y, Guiochon G. Peak parking-moment analysis. A strategy for the study of the mass-transfer kinetics in the stationary phase. *Anal Chem*. 2007;79:1970–1982.
10. Cabooter D, Lynen F, Sandra P, Desmet G. Total pore blocking as an alternative method for the on-column determination of the external porosity of packed and monolithic reversed-phase columns. *J Chromatogr A*. 2007;1157:131–141.
11. Gritti F, Guiochon G. General HETP equation for the study of mass-transfer mechanisms in RPLC. *Anal Chem*. 2006;78:5329–5347.
12. Kubin M. Beitrag zur theorie der chromatographie .2. Einfluss der diffusion ausserhalb und der adsorption innerhalb des sorbens-korns. *Coll Czech Chem Commun*. 1965;30:2900–2924.
13. Wilke C, Chang P. Correlation of diffusion coefficients in dilute solutions. *AIChE J*. 1955;1:264–270.
14. Poling B, Prausnitz J, O' Connel J. *The Properties of Gases and Liquids*, 5th ed. New York, NY: McGraw-Hill, 2001.
15. Li J, Carr P. Accuracy of empirical correlations for estimating diffusion coefficients in aqueous organic mixtures. *Anal Chem*. 1997;69: 2530–2536.
16. Gritti F, Kazakevich Y, Guiochon G. Effect of the surface coverage of endcapped C_{18}-silica on the excess adsorption isotherms of commonly used organic solvents from water in reversed phase liquid chromatography. *J Chromatogr A*. 2007;1169:111–124.
17. Knox J, McLaren L. A new gas chromatographic method for measuring gaseous diffusion coefficients and obstructive factors. *Anal Chem*. 1964;36:1477–1482.
18. Gritti F, Guiochon G. Impact of retention on Trans-column velocity biases in packed columns. *AIChE J*. In press.
19. Miyabe K, Takeuchi S. Surface diffusion of alkylbenzenes on octadecylsilyl-silica gel. *Ind Eng Chem Res*. 1998;37:1154–1158.
20. Brenner H, Gaydos L. The constrained brownian movement of spherical particles in cylindrical pores of comparable radius: models of the diffusive and convective transport of solute molecules in membranes and porous media. *J Colloid Interface Sci*. 1977;58:312–356.
21. Miyabe K, Guiochon G. Influence of column radial heterogeneity on peak fronting in linear chromatography. *J Chromatogr A*. 1999;857: 69–87.
22. Tallareck U, Albert K, Bayer E, Guiochon G. Measurement of transverse and axial apparent dispersion coefficients in packed beds. *AIChE J*. 1996;42:11, 3041–3054.
23. Farkas T, Guiochon G. Contribution of the radial distribution of the flow velocity to band broadening in hplc columns. *Anal Chem*. 1997;69:4592.
24. Abia J, Mriziq K, Guiochon G. Radial heterogeneity of some analytical columns used in high-performance liquid chromatography. *J Chromatogr A*. 1987;1218:3185–3191.
25. Gunn D. Axial and radial dispersion in fixed beds. *Chem Eng Sci*. 1987;42:363–373.
26. Hong L, Gritti F, Kaczmarski K, Guiochon G. Rate constants of mass transfer kinetics in reversed phase liquid chromatography. *AIChE J*. 2005;51:3122–3133.

Manuscript received Mar. 3, 2009, revision received Jan. 19, 2010, and final revision received Mar. 31, 2010.